Minority carrier diffusion length, lifetime and mobility in p-type GaAs and GaInAs

M. Niemeyer, J. Ohlmann, A. W. Walker, P. Kleinschmidt, R. Lang, T. Hannappel, F. Dimroth, and D. Lackner

Citation: Journal of Applied Physics **122**, 115702 (2017); doi: 10.1063/1.5002630
View online: https://doi.org/10.1063/1.5002630
View Table of Contents: http://aip.scitation.org/toc/jap/122/11
Published by the American Institute of Physics

Minority carrier diffusion length, lifetime and mobility in p-type GaAs and GaInAs

M. Niemeyer,[1,a)] J. Ohlmann,[1] A. W. Walker,[1,b)] P. Kleinschmidt,[2] R. Lang,[1] T. Hannappel,[2] F. Dimroth,[1] and D. Lackner[1]
[1]*Fraunhofer Institute for Solar Energy Systems (ISE), Heidenhofstraße 2, 79110 Freiburg, Germany*
[2]*Technische Universität Ilmenau, Institut für Physik, 98693 Ilmenau, Germany*

(Received 21 April 2017; accepted 25 August 2017; published online 19 September 2017)

Minority carrier diffusion lengths and lifetimes were determined for p-type $Ga_{(1-x)}In_xAs$ with an In-content of $0 \leq x \leq 0.53$ by cathodoluminescence and time-resolved photoluminescence measurements respectively under low injection conditions; the resulting minority carrier mobilities are also reported. Highly p-doped samples (3×10^{18} cm^{-3}) demonstrate a constant minority carrier diffusion length of (5.0 ± 0.7) μm and a constant lifetime of (3.7 ± 0.7) ns for an In-content up to 21%. Lower doped samples (3×10^{17} cm^{-3}), on the other hand, show an increase in minority carrier diffusion length and lifetime with In-content from (6.3 ± 0.2) μm and (6.2 ± 0.5) ns respectively for GaAs to (14 ± 2) μm and (24.4 ± 0.5) ns respectively for $Ga_{0.79}In_{0.21}As$. Increasing the In-content to 53% results in a drop in the minority carrier diffusion length independently of the p-doping concentration .This is interpreted as a change in the energy of the Shockley-Read-Hall trap levels within the bandgap as a function of indium concentration. *Published by AIP Publishing.*
[http://dx.doi.org/10.1063/1.5002630]

I. INTRODUCTION

The ternary alloy $Ga_{(1-x)}In_xAs$ is an interesting material for minority carrier devices like high efficiency solar cells,[1,2] photodetectors, and infrared lasers. This is due to the wide band of absorption and emission made possible by varying the composition of $Ga_{(1-x)}In_xAs$ in the range of $0 \leq x \leq 0.53$ which covers a bandgap range from 1.42 down to 0.74 eV.[3] The material can be grown lattice-mismatched on GaAs using metamorphic buffer structures or lattice-matched to InP for a composition of $Ga_{0.47}In_{0.53}As$.

Minority carrier diffusion length, lifetime and mobility are the most crucial parameters for electrical simulation and design of minority carrier devices. The diffusion lengths of $Ga_{(1-x)}In_xAs$ lattice matched to GaAs and InP[4–6] and also the lifetime of minority carriers[7,8] have both been studied extensively. These have been found to depend on several factors, including the band structure of the material, the crystal and chemical purity, as well as alloy scattering, doping, and the overall injection level. However, there exists little knowledge in the literature concerning the electrical properties of metamorphic GaInAs compounds, including minority carrier lifetime, mobility and diffusion length, considering the importance of this information for device modelling and optimization of the next generation devices.

$Ga_{(1-x)}In_xAs$ is a direct semiconductor and its diffusion length can therefore be on the order of micrometers.[9] There are several methods commonly adopted to determine such short diffusion lengths. Cross sectional electron beam induced current (EBIC) measurements are commonly performed.[10] However, the effects of surface recombination and electric fields must be properly considered in extracting solely the bulk contribution. Furthermore, EBIC measurements require several processing steps to create either a shallow *pn*-junction or a Schottky contact. Alternatively, there are two methods to determine the diffusion length of a double hetero (DH-) structure by cathodoluminescence (CL). The first method, transport imaging, requires a 2D-CCD array attached to a scanning electron microscope (SEM).[11] The other method was described by Sercel *et al.*,[12] which has several advantages over the former, including (i) simple sample preparation, (ii) no contacting of the sample for measurements, (iii) no field and surface effects and therefore an easy interpretation of results, and (iv) no 2D-CCD camera required for spatial resolution.

The minority carrier lifetime of a direct bandgap semiconductor is typically on the nanosecond scale for the doping concentrations investigated. Time-resolved photoluminescence is the preferred method and is adopted in this study. Knowing the diffusion length and the lifetime of the minority carriers enables the calculation of the minority carrier mobility at room temperature using $L = \sqrt{\tau D}$, where τ is the lifetime and D is the diffusion coefficient which is related to the mobility via the Einstein relation $D = \mu k_B T/q$.

The present paper is outlined as follows. Section II provides details concerning the samples, the processing, and the measurement setups. Section III then summarizes the measurement results, including discussion and analysis. Finally, Sec. IV provides a conclusion of the present study.

II. EXPERIMENTAL

A. Samples

Two sets of $Ga_{(1-x)}In_xAs$ DH-structures were grown in a MOVPE-system (Aixtron AIX2800-G4-TM), with TMAl,

[a)]Author to whom correspondence should be addressed: markus.niemeyer@ise.fhg.de.
[b)]Current address: National Research Council Canada, 1200 Montreal Road, M-50, Ottawa, Ontario K1A 0R6, Canada.

TMGa, TMIn, DMZn, and AsH3 as precursors. One set has a lower Zn-doping (2.5×10^{17} cm^{-3}) and another one has a higher Zn-doping (2.5×10^{18} cm^{-3}). Each set consists of 8 samples with an In-content ranging between $x = 0$ and $x = 0.53$. There are three different types of samples [labelled (i)–(iii)] in each set shown in Table I. The first type (i) includes GaAs test layers lattice matched (LM) to GaAs. In the second type (ii), the In composition is increased up to $x = 0.21$ within 5 samples ($x = 0.05, 0.07, 0.12, 0.16, 0.21$). In this set, the samples are grown on top of a step-graded metamorphic (MM) buffer described elsewhere.[13] Finally, the third type of samples (iii) has an In composition of $x = 0.53$ which is LM to InP. All samples include $Al_yGa_{(1-x-y)}In_xAs$ barriers on both sides of the GaInAs test layers with the same lattice constant. For the (i) and (ii) samples, the epitaxy was performed on GaAs wafers with a 6° offcut towards ⟨111⟩ B, whereas InP wafers with an offcut of 2° towards ⟨111⟩ B were used for type (iii) samples.

After epitaxial growth, a shading pad of aluminum (Al) [or silver (Ag)] with a thickness of 100 nm [or 200 nm, respectively] is evaporated onto the parts of the sample, leading to a shadow mask with a sharp edge. The extracted diffusion length does not show dependence on the type of metal or on the metal pad thickness. The extraction method is explained later.

B. Time resolved photoluminescence setup and measurement procedure

The effective minority carrier lifetime was measured by the method of time-resolved photoluminescence. The DH-structures were excited by pulsed laser light employing a 640 nm diode laser (PicoQuant). The decay of the radiative band-to-band recombination was measured by a single photon counting avalanche photodiode (id Quantique), or, for photon energies below 1.37 eV, by an InGaAs photomultiplier tube (Hamamatsu H10330A-75), fed into a time-correlated single photon counting unit (PicoHarp 300). The excitation density was calculated from the effective excitation volume, the repetition rate of the laser and the laser power measured by a photodiode at the position of the sample. The overall time resolution given by the width of the system response function was on the order of 150 ps in the case of detection by the avalanche photodiode, increasing to 500 ps when using the photomultiplier tube. The photoluminescence signal was measured from each sample for several excess carrier densities between 10^{12} cm^{-3} and 10^{15} cm^{-3}, respectively. The effective lifetime was extracted from the measured decay by fitting an exponential decay function. However, the excess carrier density is not constant during a single TR-PL measurement. Therefore, the lifetime extracted from the PL signal is only valid if it is constant within the measured range of excess carrier density. For the samples discussed, this is achieved for low excess carrier densities of $\Delta n \leq 10^{13}$ cm^{-3}, since both the radiative and SRH lifetimes are constant as Δn is negligible compared to the doping density N and since the SRH process is dominated by the captures of minority carriers.

C. Cathodoluminescence setup and measurement procedure

The CL-signal was measured in an electron microscope (Hitachi, SU 70) featuring an integrated commercially available CL-setup (Gatan, MonoCL3). Excitation by the electron beam is done in a spatially resolved manner. Panchromatic detection over the whole sample was performed without spatial resolution. The electron beam is moved perpendicular to the metal edge while the CL signal intensity is measured by either a GaAs photo-multiplier tube (Hamamatsu, R374) for GaAs test layers or an extended GaInAs diode (Hamamatsu, G7754-01) for ternary $Ga_{(1-x)}In_xAs$ test layers. Figure 1 (left) illustrates a schematic of the sample structure, the electron beam and the metal edge.

The excitation volume of minority carriers inside the sample is simulated with CASINO,[14] a Monte Carlo simulation based software. The xz-plane of a 10 kV electron beam is shown in Fig. 1 (right), where the simulated lateral full-width at half-maximum is less than 200 nm. For diffusion lengths longer than 1 μm, the measured diffusion length is not significantly influenced by the excitation volume and can therefore be neglected.

The CL signal is integrated over at least 2 ms for each data point. This is several orders of magnitude longer than the expected minority carrier lifetime in GaAs of about 10 ns.[15,16] The measurement result can therefore be assumed to be time-independent. Solving the continuity equation, the decline of the CL signal $C(A, L_D)$, moving the electron beam from the metal edge to the metal, is an exponential decay and expressed as[12]

TABLE I. Layer sequences of the three types of DH-test-structures. "LM" stands for lattice matched on (i) GaAs and (iii) on InP, whereas "MM" stands for metamorphic GaInAs with an In-content of $0 \leq x \leq 0.21$ grown on different metamorphic GaInAs buffer structures on GaAs wafers (ii). Barriers and test layers are p-type with a doping concentration between 1×10^{17} and 2.5×18 cm^{-3}, except for the cap layer which was not intentionally doped (nid). Structure (i) has a 9× $Ga_{0.60}In_{0.40}P$(50 nm)-$Ga_{0.85}In_{0.15}As$ (33 nm) strain balanced absorber structure between the lower barrier and the substrate to suppress photon coupling between the test layer and the substrate.

	LM on GaAs (i)	MM on GaAs (ii)	LM on InP (iii)	Thickness (nm)	Zn-Doping (cm^{-3})
Cap	GaAs	GaAs		10	nid
Barrier	$Al_{0.70}Ga_{0.30}As$	$Al_{0.50}Ga_{(0.50-y)}In_xAs$	$Al_{0.47}In_{0.53}As$	50	10^{17}
Test layer	GaAs	$Ga_{(1-x)}In_xAs$	$Ga_{0.47}In_{0.53}As$	1000	$2.5 \times 10^{17}/2.5 \times 10^{18}$
Barrier	$Al_{0.70}Ga_{0.30}As$	$Al_{0.50}Ga_{(0.50-y)}In_xAs$	$Al_{0.47}In_{0.53}As$	100	10^{17}
	9× $Ga_{0.60}In_{0.40}P$-$Ga_{0.85}In_{0.15}As$	Metamorphic GaInAs Buffer			nid
Substrate	GaAs (si)	Virtual Substrate	InP		

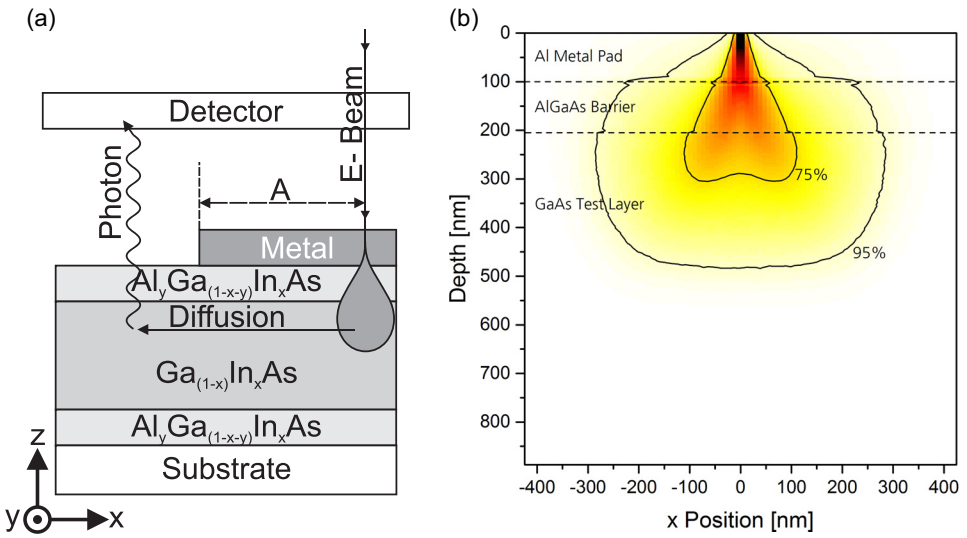

FIG. 1. Left: Sketch of the measurement method. The electron beam is focused onto the metal at a distance A from the metal edge. Electron energy is partially absorbed in the metal layer (compare figure on the right), but most of the energy is deposited on the $Ga_{(1-x)}In_xAs$ test layer by creating electron-hole pairs. The detector integrates the cathodoluminescence signal emitted by minority carriers which have diffused from the point of excitation to a position not shaded by the metal. The CL signal is measured as a function of distance A without spatial resolution. Right: Energy distribution in an *xz*-plane for a 10 kV electron beam in the test structure. The area in which 75% (95%) of the energy in the plane is deposited is marked (black line).

$$C(A, L_D) = c_0\, e^{-A/L_D}, \tag{1}$$

where c_0 is a normalization constant, L_D is the minority carrier diffusion length, and A is the distance between the electron beam and the metal edge.

All samples were characterized at room temperature using an electron beam of 150 pA with an acceleration voltage of 10 kV. Since the excess carrier density is not constant in the area from which the signal is integrated, an excitation beam resulting in low injection is necessary, since this is a measurement regime where the diffusion length is not dependent on excess carrier density. The excess carrier density injected into the test layer can be calculated assuming a point excitation and constant excess carrier density as a function of depth (since the diffusion length is significantly longer than the sample thickness). It decreases with the distance to the electron beam. The starting point of the exponential fit to calculate the diffusion length was set at a distance of 0.5 μm between the electron beam and the metal edge. Therefore, the excess carrier density at this distance is calculated in the following.

The simulation of the electron beam [see Fig. 1 (right)] indicates that 29% of the electrons are reflected at the surface and 44% of the electron beam energy is deposited on the test layer. For the sample thickness, measured lifetime and diffusion length from the exponential fit, and assuming that the generation of an electron-hole pair in GaAs requires an energy of 4.6 eV,[17,18] one can solve the diffusion equation in 2D, which leads to a Bessel function and determine the excess carrier density to be below $10^{14}\,\mathrm{cm}^{-3}$. This satisfies the low injection criteria, since the injected carrier density is very small compared to the doping level ($\geq 2.5 \times 10^{17}\,\mathrm{cm}^{-3}$) for all the test structures.

Each sample is measured at a minimum of three positions on a quarter piece of a 4″ wafer. One measurement consists of 256 line scans over approximately 60 μm distance along the metal edge. As an example, a line scan is shown in Fig. 2. The error in the extracted diffusion length is calculated using the standard deviation over all line scans. In addition, the doping level was measured for each sample by electrochemical capacitance-voltage (ECV) profiling to ensure that the luminescence intensity is not influenced by a variation in doping.

Test layer thicknesses between 200 and 2000 nm did not show any measurable effect on the diffusion length. This was tested for both, GaAs and $Ga_{0.47}In_{0.53}As$ samples, and was confirmed that interface recombination is not significant. In fact, the diffusion length of minority carriers in our samples is dominated by the specific material properties of the bulk test layer.

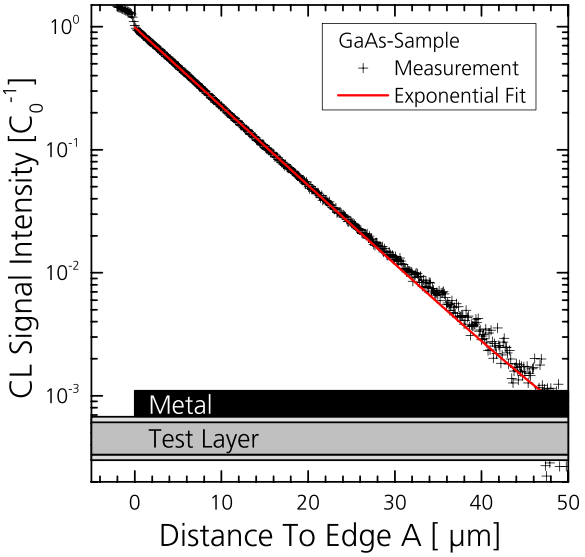

FIG. 2. Measured CL signal intensity (crosses) as a function of the distance between the electron beam and the metal edge. The measurement was performed on a GaAs sample and the dataset was fit to Eq. (1) shown as the red solid line.

All metamorphic test layers were grown fully unstrained on buffer structures, as verified by high resolution XRD reciprocal space maps. As a result, no misfit dislocations are visible in the CL images from the test layers, since they are confined to the metamorphic buffer below the test layer which does not contribute to the CL signal. However, threading dislocations are detected in the test layer, originating from the growth of the metamorphic buffer structure. The measured threading dislocation density (TDD) increases with lattice mismatch and therefore with In-content. The highest TDD of 8×10^5 cm^{-2} was measured for the $Ga_{0.79}In_{0.21}As$ test layer with the highest lattice mismatch to GaAs (see Fig. 3). The exponential decline of the CL signal as a function of the distance from the metal edge is not significantly influenced for TDDs in the 10^5 cm^{-2} range. A single line scan of the CL signal which scans in the vicinity of a threading dislocation will show anomalous signal decay, but averaging 256 lines removes such anomalous results. This is confirmed by the consistency of many measurements at different positions of the same sample. However, it is still important to monitor the density of dislocations in each test sample because the combination of high TDD and long diffusion length increases the uncertainty and local fluctuations appear between measurement results.

III. RESULTS AND DISCUSSION

Figure 4 shows the diffusion length, extracted from the CL decay of various $Ga_{(1-x)}In_xAs$ samples, as a function of the In-content and for two p-doping levels, 2.5×10^{17} and 2.5×10^{18} cm^{-3}. An increase in uncertainty with increasing lattice mismatch to GaAs is visible in Fig. 4, which is due to the increasing impact of the threading dislocations on the measurement and the associated fitting.

A clear trend is observed for the two sets of $Ga_{(1-x)}In_xAs$ structures with different p-doping levels. The diffusion length

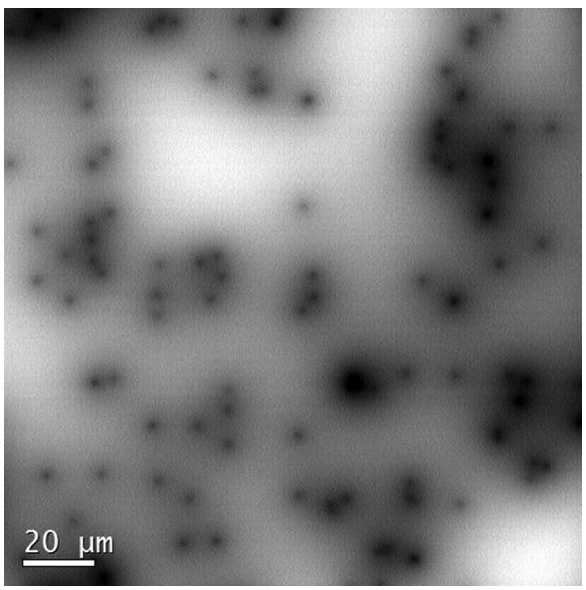

FIG. 3. Plain view CL image of the $Ga_{0.79}In_{0.21}As$ sample without metal layers for the determination of the threading dislocation density (TDD). Dark areas show threading dislocations (TD). The TDD was determined to be 8×10^5 cm^{-2} for this sample.

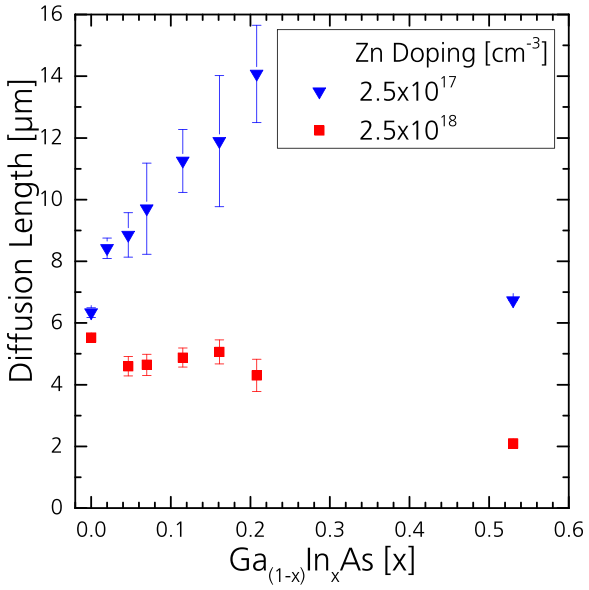

FIG. 4. Minority carrier diffusion lengths in $Ga_{(1-x)}In_xAs$ for x ranging from 0 to 0.53 for two p-doping concentrations. For samples with a p-doping concentration of $(2.5 \pm 0.5) \times 10^{18}$ cm^{-3} (red squares) and a doping concentration of $(2.5 \pm 0.5) \times 10^{17}$ cm^{-3} (blue triangles).

of all samples with the higher p-doping of $(2.5 \pm 0.5) \times 10^{18}$ cm^{-3} is in the range of 4–5 μm and is nearly constant over In-content between 0 and 21%, dropping only to 2 μm for the $Ga_{0.47}In_{0.53}As$ sample with a significantly higher In-content of 53%. Samples with the lower p-doping of $(2.5 \pm 0.5) \times 10^{17}$ cm^{-3} show a linear increase in diffusion length from 6 to 14 μm for an In-content increasing from 0 to 21%. However, the $Ga_{0.47}In_{0.53}As$ sample with the highest In-content has again a shorter diffusion length of 7 μm. The measured diffusion lengths are in good agreement with the values reported in the literature for GaAs[4] and $Ga_{0.47}In_{0.53}As$.[5,6] In order to gain insight into these trends, one must investigate the nature of these diffusion lengths. This increase in diffusion length can be a result of an increase in lifetime, an increase in mobility, or both.

The minority carrier lifetime is investigated via TR-PL, with the results illustrated in Fig. 5. The lifetime is nearly constant with In-content for the samples with the higher p-doping concentration (2.5×10^{18} cm^{-3}). However, the lifetime in the samples with the lower p-doping concentration (2.5×10^{17} cm^{-3}) is increasing with In-content. This observation supports the measured increase in the diffusion length from Fig. 4.

Prior to discussing the lifetime results, the minority carrier mobility is calculated using Eq. (2). The results are shown in Fig. 6. Both sets of samples show constant minority carrier mobility with In-content within the measurement uncertainty. A minority carrier mobility of (3800 ± 800) cm^2/Vs is measured for the lower doped samples, and a slightly lower minority carrier mobility of (2300 ± 600) cm^2/Vs is measured for the higher doped samples. The measured minority carrier mobility in GaAs is in good agreement with the measured ones by Ito *et al.*[19] With respect to the ternary alloy, there is no published data for the mobility of minority carriers to our knowledge. However, the majority Hall electron mobility can

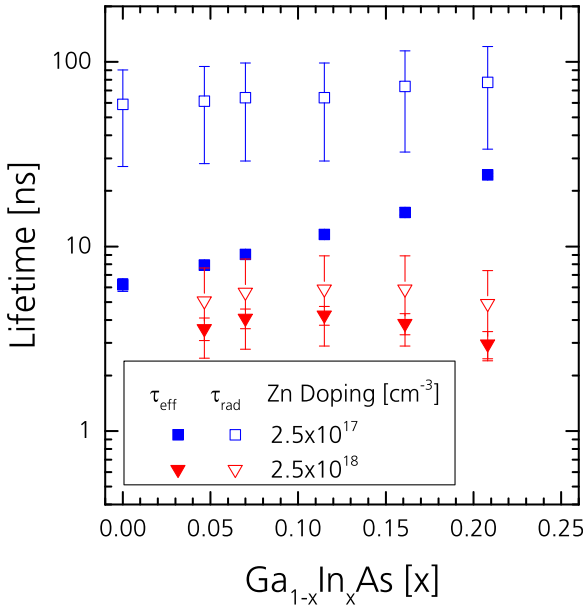

FIG. 5. Minority carrier lifetime in $Ga_{1-x}In_xAs$ DH-structures determined from TR-PL measurements (filled symbols) and calculated radiative lifetime (open symbols) at low injection for two p-doping concentrations in the test layer: $(2.5 \pm 0.5) \times 10^{17}$ cm^{-3} (blue triangles) and $(2.5 \pm 0.5) \times 10^{18}$ cm^{-3} (red squares).

be used as an initial guess. For $Ga_{(1-x)}In_xAs$, it is simulated using the model from Chattopadhyay *et al.*[20] for an *n*-doping concentration of $n = 2.3 \times 10^{17}$ cm^{-3}. The electron Hall mobility remains nearly constant at $(4500 \pm 200) \times 10^3$ cm^2 V^{-1} s^{-1} as a function of In-content due to alloy scattering, and increasing beyond $x = 0.20$ up to 6000 cm^2 V^{-1} s^{-1}.[20] This supports the measured constant mobility with In-content in the range of $0 \leq x \leq 0.2$ for the two p-doping levels reported here.

The explanation for an increase in diffusion length is therefore the measured increase in lifetime. There are three

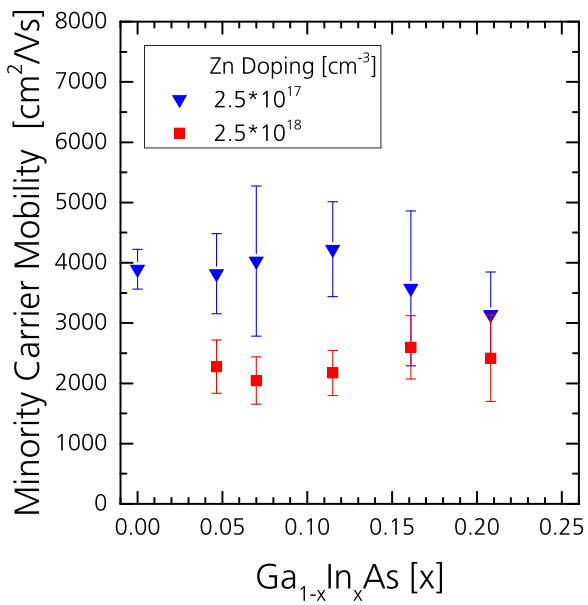

FIG. 6. Minority carrier mobility of GaInAs for two p-doping concentrations in the test layer: $(2.5 \pm 0.5) \times 10^{17}$ cm^{-3} (blue triangles) and $(2.5 \pm 0.5) \times 10^{18}$ cm^{-3} (red squares). Values are calculated from TR-PL lifetimes and CL diffusion lengths at low injection.

recombination mechanisms which dictate the measured lifetime: radiative (τ_{rad}), Shockley-Read-Hall (τ_{SRH}) and Auger (τ_{Aug}), where the effective lifetime τ_{eff} can be calculated as

$$\frac{1}{\tau_{eff}} = \frac{1}{\tau_{SRH}} + \frac{1}{\tau_{rad}} + \frac{1}{\tau_{Aug}}. \quad (2)$$

Since the Auger coefficient for GaAs has been measured to be $(7 \pm 4) \times 10^{-30}$ cm^6 s^{-1},[21] and the Auger coefficient for $Ga_{0.47}In_{0.53}As$ has been calculated to be 4×10^{-30} cm^6 s^{-1},[22] the Auger recombination can be deemed negligible compared to the radiative recombination for doping levels below 10^{19} cm^{-3} and low injection measurement conditions. This is the case for both sets of samples. The remaining lifetimes which are expected to dominate under low level injection are thus radiative and SRH.

The radiative recombination lifetime at low injection is inversely proportional to the product of the doping and the radiative recombination coefficient B_{rad} as $\tau_{rad} = 1/[(1-f)B_{rad}N]$,[23] where f is the photon recycling factor. This photon recycling factor accounts for the re-absorption of photons emitted in the test layer, which results in a longer observed lifetime; this factor depends primarily on the test layer thickness. Since the layer thicknesses are kept constant for all samples, we can assume little variation in f between all samples.

The radiative recombination coefficient for GaAs has been calculated[24] and measured[21] to be about 2×10^{-10} cm^3 s^{-1} at room temperature. The radiative recombination coefficient of $Ga_{0.47}In_{0.53}As$ has also been measured to be about 1.4×10^{-10} cm^3 s^{-1},[7] which implies that the coefficient does not change significantly over this range of In-content, unless strong bowing occurs. To explore this possibility further, the calculation of B_{rad} based on measured photon absorption data for $Ga_{0.71}In_{0.19}As$ was conducted following the procedure described in Ref. 15 for a metamorphic $Ga_{0.71}In_{0.19}As$ solar cell presented in Ref. 25. The result is a B_{rad} of 1.0×10^{-10} cm^3 s^{-1}, which supports the hypothesis that the B_{rad} and therefore the radiative lifetime remain constant with In-concentration. Assuming a constant B_{rad} of $(2 \pm 1) \times 10^{-10}$ cm^2/s with In-content and a photon recycling factor of 0.66 as in 1 μm thick GaAs samples[26] and measuring the doping concentration via ECV, the radiative lifetime is estimated for all samples and is shown in Fig. 5 as open symbols. With respect to the higher doped samples, the radiative lifetime is estimated to be 6 ± 3 ns for these samples. This is just slightly longer than the measured effective lifetimes of 3.5 ± 0.7 ns and well within the measurement uncertainty shown in Fig. 5. Thus, the higher doped samples are dominated by radiative recombination.

Finally, the Shockley-Read-Hall (SRH) recombination lifetime must be considered as a function of In-content. Since SRH recombination is trap-assisted, it thus depends on the trap concentration in the crystal, its energetic position with respect to the valence band, and the capture cross-section for electrons and holes. The traps can be either intrinsic bulk defects or introduced by dopants. Bulk defects have been previously shown to limit the lifetime in the range of low doping ($<10^{18}$ cm^{-3}).[27] At higher doping levels, the trap concentration may depend on the dopant type and

concentration as well as growth conditions in the reactor, including temperature, growth rate, III/V ratio, etc.

The traps which are most efficient in recombining both carrier types lie close to the middle of the bandgap. By changing the material composition of $Ga_{(1-x)}In_xAs$, the bandgap changes and thus the position of the defects within the bandgap can be expected to change as well. A possible explanation for the observed increase in diffusion length with In-content for the lower doped samples (see Fig. 4), considering the radiative lifetime is constant and an increase in lifetime is measured (see Fig. 5), is a shift of the energy levels of bulk defects away from the middle of the bandgap, resulting in an increased SRH lifetime as a function of In-content. However, this is yet to be confirmed, and further investigations are required using deep-level transient spectroscopy for example.

IV. CONCLUSIONS

The minority carrier diffusion length, lifetime and mobility of *p*-type $Ga_{1-x}In_xAs$ were investigated in the composition range between $x = 0$ and $x = 0.53$ for test structures with two different Zn doping levels of 2.5×10^{17} cm^{-3} and 2.5×10^{18} cm^{-3}. This analysis was performed for various metamorphic $Ga_{(1-x)}In_xAs$ compositions which were grown fully relaxed on buffer structures on GaAs. This opens a source of important minority carrier transport properties for the ternary alloy which were previously inaccessible. The minority carrier diffusion length was determined by fitting the measured luminescence of double-hetero structures using an electron microscope. It was shown that a threading dislocation density of up to 8×10^5 cm^{-2} in the metamorphic layers does not significantly influence the measured diffusion length for the given samples and the measurement method. For samples with a p-doping level of 2.5×10^{17} cm^{-3}, the diffusion length was found to first increase with In-content from (6.3 ± 0.2) μm for GaAs to (14 ± 2) μm for $Ga_{0.79}In_{0.21}As$ and subsequently drop to (4.7 ± 0.2) μm for $Ga_{0.47}In_{0.53}As$. Samples with a higher p-doping level of (2.5×10^{18} cm^{-3}) did not show a significant dependence of the minority carrier diffusion length on the In-content, with a diffusion length constant in the range of (5.0 ± 0.7) μm.

The minority carrier lifetimes for the same samples were determined using time-resolved photoluminescence under low injection conditions. Lifetimes increased both significantly and monotonically for the samples with the lower p-doping concentration of 2.5×10^{17} cm^{-3} from (6.2 ± 0.5) ns for $x = 0$ to (24.4 ± 0.5) ns for $x = 0.21$. For the samples with a p-doping of 2.5×10^{18} cm^{-3}, a constant lifetime of (3.7 ± 0.7) ns was measured.

Combining the measured diffusion length with the measured lifetime yielded the minority carrier mobility, which was found to be constant with In-content, but showed a dependence on doping, as expected. The observed increase in diffusion length is then a result of the increased lifetime, for which SRH recombination lifetime is identified as the explanation. The leading hypothesis is that the traps with the highest capture cross-section are situated further from the middle of the bandgap as the In-content is increased. However, these must become more efficient for $Ga_{0.47}In_{0.53}As$ lattice matched to InP, since the diffusion length decreases considerably at this composition.

ACKNOWLEDGMENTS

This work has received funding from the European Union's Horizon 2020 research and innovation programme within the project CPVMatch under Grant Agreement No. 640873. The authors would like to thank S. Stättner, M. Scheer, and K. Wagner for their technical support on the metal organic vapor phase epitaxy reactor, and R. Koch and A. Schütte for the evaporation of the metal films. M. Niemeyer acknowledges the scholarship support from the German Federal Environmental Foundation (DBU).

[1]R. M. France, J. F. Geisz, I. Garcia, M. A. Steiner, W. E. McMahon, D. J. Friedman, T. E. Moriarty, C. Osterwald, J. Scott Ward, A. Duda, M. Young, and W. J. Olavarria, IEEE J. Photovoltaics **5**, 432 (2015).
[2]A. W. Bett, S. P. Philipps, S. Essig, S. Heckelmann, R. Kellenbenz, V. Klinger, M. Niemeyer, D. Lackner, and F. Dimroth, "Overview about technology perspectives for high efficiency solar cells for space and terrestrial applications," in *28th European Photovoltaic Solar Energy Conference and Exhibition* (Paris, September 2013).
[3]K. Goetz, D. Bimberg, H. Jürgensen, J. Selders, A. V. Solomonov, G. F. Glinskii, and M. Razeghi, J. Appl. Phys. **54**, 4543 (1983).
[4]H. C. Casey, Jr., B. I. Miller, and E. Pinkas, J. Appl. Phys. **44**, 1281 (1973).
[5]M. M. Tashima, L. W. Cook, and G. E. Stillman, J. Electron. Mater. **11**, 831 (1982).
[6]Y. Takeda, M. Kuzuhara, and A. Sasaki, Jpn. J. Appl. Phys., Part 1 **19**, 899 (1980).
[7]R. K. Ahrenkiel, R. Ellingson, S. Johnston, and M. Wanlass, Appl. Phys. Lett. **72**, 3470 (1998).
[8]R. K. Ahrenkiel, R. Ellingson, S. Johnston, J. Webb, J. Carapella, and M. Wanlass, in *Fourth NREL Conference on Thermophotovoltaic Generation of Electricity* (AIP, 1999), pp. 282–288.
[9]E. Vigil and P. Diaz, Cryst. Res. Technol. **19**, 285 (1984).
[10]D. E. Ioannou and C. A. Dimitriadis, IEEE Trans. Electron Devices **29**, 445 (1982).
[11]D. R. Luber, F. M. Bradley, N. M. Haegel, M. C. Talmadge, M. P. Coleman, and T. D. Boone, Appl. Phys. Lett. **88**, 163509 (2006).
[12]P. C. Sercel, H. A. Zarem, J. A. Lebens, L. E. Eng, A. Yariv, and K. J. Vahala, in *International Technical Digest on Electron Devices Meeting* (1989), pp. 285–288.
[13]J. Ohlmann, M. Niemeyer, R. Lang, F. Dimroth, and D. Lackner, *Empirical Strain-Thickness-Model for Metamorphic Ga1-xInxAs-Buffer Structures* (Lund, Sweden, 2015).
[14]P. Hovington, D. Drouin, and R. Gauvin, Scanning **19**, 1–14 (1997).
[15]A. W. Walker, S. Heckelmann, C. Karcher, O. Höhn, C. Went, M. Niemeyer, A. W. Bett, and D. Lackner, J. Appl. Phys. **119**, 155702 (2016).
[16]S. Tiwari and S. L. Wright, Appl. Phys. Lett. **56**, 563 (1990).
[17]B. G. Yacobi and D. B. Holt, *Cathodoluminescence Microscopy of Inorganic Solids* (Plenum Press, New York, New York, USA, 1990).
[18]C. A. Klein, J. Appl. Phys. **39**, 2029 (1968).
[19]H. Ito and T. Ishibashi, J. Appl. Phys. **65**, 5197 (1989).
[20]D. Chattopadhyay, S. K. Sutradhar, and B. R. Nag, J. Phys. C: Solid State Phys. **14**, 891 (1981).
[21]U. Strauss, W. W. Rühle, and K. Köhler, Appl. Phys. Lett. **62**, 55 (1993).
[22]D. Steiauf, E. Kioupakis, and C. G. Van de Walle, ACS Photonics **1**, 643 (2014).
[23]M. P. Lumb, M. A. Steiner, J. F. Geisz, and R. J. Walters, J. Appl. Phys. **116**, 194504 (2014).
[24]F. Stern, J. Appl. Phys. **47**, 5382 (1976).
[25]M. Niemeyer, V. Klinger, F. Dimroth, F. Predan, P. Fuss-Kailuweit, D. Reinwand, D. Lackner, A. Wekkeli, E. Oliva, M. Schachtner, G. Siefer, and A. W. Bett, in *29th European Photovoltaic Solar Energy Conference and Exhibition* 1991–1995 (2014), p. 5.
[26]M. P. Lumb, M. K. Yakes, M. Gonzalez, R. Hoheisel, C. G. Bailey, W. Yoon, and R. J. Walters, "Development of tunnel junctions with high peak tunneling currents for InP-based multijunction solar cells," in *Proceedings of the 38th IEEE Photovoltaic Specialists Conference* (2012), pp. 949–953.
[27]H. Ito, T. Furuta, and T. Ishibashi, Appl. Phys. Lett. **58**, 2936 (1991).